0026-895X/07/7202-370–379
MOLECULAR PHARMACOLOGY
U.S. Government work not protected by U.S. copyright
Mol Pharmacol 72:370–379, 2007

Vol. 72, No. 2
35394/3227633
Printed in U.S.A.

5-Androstenediol Promotes Survival of γ-Irradiated Human Hematopoietic Progenitors through Induction of Nuclear Factor-κB Activation and Granulocyte Colony-Stimulating Factor Expression

Mang Xiao, Cynthia E. Inal, Vaishali I. Parekh, Cheng-Min Chang, and Mark H. Whitnall

Radiation Countermeasures Program, Armed Forces Radiobiology Research Institute, Uniformed Services University of the Health Sciences, Bethesda, Maryland

Received February 27, 2007; accepted May 1, 2007

ABSTRACT

5-Androstenediol (5-AED) stimulates hematopoiesis and enhances survival in animals exposed to ionizing radiation (IR), suggesting that this steroid may act on hematopoietic progenitor cells. We used γ-irradiated primary human CD34$^+$ hematopoietic progenitor cells to show that 5-AED protects hematopoietic cells from IR damage, as shown by enhanced cell survival, clonogenicity, proliferation, and differentiation. Unlike in tumor cells, IR did not induce nuclear factor-κB (NFκB) activation in primary progenitors. However, IR stimulated IκB$_\beta$ release from NFκB/IκB complexes and caused NFκB1 (p50) degradation. 5-AED stabilized NFκB1 in irradiated cells and induced NFκB gene expression and NFκB activation (DNA binding). 5-AED stimulated interleukin-6 and granulocyte colony-stimulating factor (G-CSF) secretion. The survival-enhancing effects of 5-AED on clonogenic cells were abrogated by small interfering RNA inhibition of NFκB gene expression and by neutralization of G-CSF with antibody. The effects of 5-AED on survival and G-CSF secretion were blocked by the NFκB inhibitor *N*-benzoyloxycarbonyl (*Z*)-Leu-Leu-leucinal (MG132). 5-AED had no effect on accumulation of the proapoptotic factor p53 after IR, as determined by Western blot. The results indicate that NFκB1 degradation after IR may be responsible for the radiation sensitivity of CD34$^+$ cells compared with tumor cells. 5-AED exerts survival-enhancing effects on irradiated human hematopoietic progenitor cells via induction, stabilization, and activation of NFκB, which results in increased secretion of hematopoietic growth factor G-CSF.

5-Androstenediol (5-androstene-3β-17β-diol, 5-AED) a novel nontoxic radiation countermeasure, enhances survival in mice and monkeys exposed to whole-body γ-IR (Whitnall et al., 2005; Stickney et al., 2006, 2007) and induces hematopoiesis and hematopoietic growth factor expression (Whitnall et al., 2000; Singh et al., 2005; Stickney et al., 2006, 2007). 5-AED administration causes increases in circulating granulocytes, monocytes, NK cells, and platelets in irradiated animals (Whitnall et al., 2000; Stickney et al., 2007). 5-AED also displays beneficial effects after burn injury, trauma, and sepsis (Szalay et al., 2006). However, the mechanisms of action of 5-AED are not well understood. Injury after prompt IR of hematopoietic tissue is caused by apoptosis in hematopoietic stem and progenitor cells occurring over a period of hours to days. The moderate dose range (1–7 Gy in humans) of exposures to ionizing radiation poses a risk of damage to the hematopoietic system (Coleman et al., 2004) and results in mortality caused by opportunistic infection and hemorrhage. Hence, investigation of the signaling pathways involved in IR-induced apoptosis in human primary hematopoietic cells and the possible modulation of apoptotic pathways by radiation countermeasures is central to understanding the mechanisms of action of these agents.

NFκB is a dimeric DNA-binding protein of the Rel/NFκB family, which consists of five members (c-Rel, p65/RelA, RelB, p50, and p52). The p65/p50 heterodimer is the most common form in mammalian cells, and this is what is commonly referred to as "NFκB" (Pahl, 1999; Karin and Ben-

National Institute of Allergy and Infectious Diseases Interagency Agreement Y1-AI-3809-01 to Armed Forces Radiobiology Research Institute, Henry M. Jackson Foundation award 52762 (to M.H.W.), and Department of Defense Peer-Review Medical Research Program grant PR054180 (to M.H.W.).

Article, publication date, and citation information can be found at http://molpharm.aspetjournals.org.

doi:10.1124/mol.107.035394.

ABBREVIATIONS: 5-AED, 5-androstenediol; IR, ionizing radiation; NFκB, nuclear factor κB; G-CSF, granulocyte colony-stimulating factor; IL, interleukin; MG132, *N*-benzoyloxycarbonyl (*Z*)-Leu-Leu-leucinal; siRNA, small interfering RNA; IMDM, Iscove's modified Dulbecco's medium; rh, recombinant human; SCF, stem cell factor; 7AAD, 7-aminoactinomycin D; PCR, polymerase chain reaction; QRT-PCR, quantitative real-time polymerase chain reaction; ELISA, enzyme-linked immunosorbent assay; IP, immunoprecipitation; DNA-PK, DNA-dependent protein kinase.

Neriah, 2000). The Rel/NFκB complexes are retained in cytoplasm by inhibitors of the IκB family. Various stimuli, such as ultraviolet radiation, IR, and free radicals, induce IκB phosphorylation and degradation through ubiquitin/proteasome pathways. The released NFκB translocates into the nucleus, binds to target DNA, and initiates transcription. NFκB is known to promote the expression of target genes that regulate immune responses, stress responses, and cell growth or survival (Thompson et al., 1995; Joyce et al., 2001).

NFκB expression has been found in human fetal blood hematopoietic stem and progenitor $Lin^{-}CD34^{+}CD38^{-}$ cells (Shojaei et al., 2004), and in $CD34^{+}CD19^{-}$ bone marrow cells and is required for $CD34^{+}$ cell clonogenic function and survival (Pyatt et al., 1999). Recent studies indicated that tumor cells usually possess high levels of constitutive NFκB activity. Exposure of these cells to IR increases NFκB activity (Kim et al., 2005; Braun et al., 2006). This disordered constitutive NFκB activity plays an important role in radioresistance of malignant cells; therefore, inhibiting NFκB activity has been proposed as a cancer therapy strategy (Luo et al., 2005; Magné et al., 2006). However, NFκB also modulates IR-induced damage in normal human tissue, and levels of this factor in human primary $CD34^{+}$ cells are relatively low (Pyatt et al., 1999; Guzman et al., 2001; Romano et al., 2003). Furthermore, baseline NFκB expression levels are lower in human $CD34^{+}$ cells than all mature hematopoietic cell lineages (Griffin et al., 1989; Granelli-Piperno et al., 1995; McDonald et al., 1997). NFκB is activated by cytokines and is known to regulate hematopoiesis. Hence, low NFκB expression may be related to the high radiation sensitivity of hematopoietic progenitor cells (Besançon et al., 1998; Pyatt et al., 1999).

To examine the effects of IR on human stem and progenitor cells, to evaluate the usefulness of 5-AED as a radiation countermeasure for human cells, and to test hypotheses concerning signaling pathways mediating these effects, we administered 5-AED to γ-irradiated human primary $CD34^{+}$ cells, a population comprising pluripotent hematopoietic stem cells and lineage-committed hematopoietic progenitors. The present results demonstrate that 5-AED can act directly on cells from hematopoietic tissue and that direct cellular targets of 5-AED include one or more of the hematopoietic subpopulations contained within $CD34^{+}$ cells.

Materials and Methods

Drug Preparation. 5-AED (androst-5-ene-3β, 17β-diol) was purchased from Steraloids (Wilton, NH) and was freshly prepared and administered at 1 μg/ml based on our preliminary data. Because 5-AED is insoluble in aqueous media, 20 mg of 5-AED was added to 2 ml of dimethyl sulfoxide, and sonicated in a 45°C water bath until completely dissolved. The 5-AED/dimethyl sulfoxide solution was diluted in 10% fetal bovine serum to achieve the 100× stock solution. Vehicle controls were used in all experiments (Whitnall et al., 2000).

Cell Culture, Cytokines, IR, and Drug Treatment. Human $CD34^{+}$ cells were provided by the National Hematopoietic Cell Processing Core directed by Dr. Shelly Heimfeld (Fred Hutchinson Cancer Research Center, Seattle, WA) (Elagib et al., 2004). Thawed $CD34^{+}$ cells were cultured in serum-free medium consisting of Iscove's modified Dulbecco's medium (IMDM) supplemented with BIT 9500 (Stem Cell Technologies, Tukwila, WA) and penicillin/streptomycin. Recombinant human (rh) stem cell factor (SCF; 100 ng/ml), rh flt-3 ligand (100 ng/ml), and rh interleukin-3 (IL-3; 25 ng/ml) were added. All cytokines were purchased from PeproTech, Inc. (Rocky Hill, NJ). $CD34^{+}$ cells were γ-irradiated at doses of 0, 2, 4, or 6 Gy (0.6 Gy/min) in the Armed Forces Radiobiology Research Institute Cobalt facility 72 h after thawing. After IR, cells were washed with serum-free medium once, and fresh culture medium with the above cytokines and factors was added. Incubations of cells in 5-AED were for the 24-h period before IR, the 24 h period after IR or both before and after IR. MG132 (Calbiochem, La Jolla, CA) (0.1–0.5 μM) was added 1 h before IR to $CD34^{+}$ cultures with and without 5-AED administration in indicated experiments (Romano et al., 1999; Guzman et al., 2001).

Flow Cytometry and Clonogenic Assays. Cell expansion and viability (trypan blue-negative cells) from all groups were counted. Death and apoptotic markers and cell lineage-specific surface phenotypes were determined using BD FACS Caliber flow cytometry (BD Biosciences, San Jose, CA). All antibodies and dyes including anti-CD34, anti-CD11b, Annexin-V, and 7-aminoactinomycin D (7AAD) or propidium iodide were purchased from BD Biosciences (Xiao et al., 2001; Dooley et al., 2004).

Committed hematopoietic progenitors in the $CD34^{+}$ population were quantitated in standard semisolid cultures in triplicate using 1 ml of Methocult GF+ (Stem Cell Technologies), which consists of 1% methylcellulose in IMDM, 30% fetal bovine serum, 1% bovine serum albumin, 2 mM L-glutamine, 10^{-5} M 2-mercaptoethanol, 50 ng/ml SCF, 20 ng/ml granulocyte macrophage–colony-stimulating factor, 20 ng/ml G-CSF, 20 ng/ml IL-3, and 3 U/ml erythropoietin. Cells from liquid culture were washed twice with IMDM before assays and seeded with 1 to 5 × 10^{3} cells/dish in 35-cm cell culture dishes (from BD Biosciences). Plates were scored for erythroid, granulocyte-macrophage, and mixed-lineage colonies after culturing for 14 days at 37°C/5% CO_2 (Elagib et al., 2004).

Quantitative Real-Time PCR. Total RNA was extracted from 1 × 10^{4} total cultured cells using RNAqueous-4PCR Kits from Ambion (Austin, TX) and was reverse-transcribed using random hexamers according to the manufacturer's instructions (Bio-Rad Laboratories, Hercules, CA). Gene sequences were obtained from GenBank. Primers and probes for all target gene sequences were designed using the computer program Beacon Designer (Premier, Palo Alto, CA). Multiplex quantitative real-time PCR (QRT-PCR) assays were carried out using cDNA, primers (human IL-6, G-CSF, NFκBp65 and p50, and 18S rRNA subunit, which was used as an internal control), fluorogenic probes, and iQ Supermix (Bio-Rad Laboratories). The fluorochromes used in this study were 6-carboxyfluorescein, hexachloro-6-carboxyfluorescein, Cy 5, and Texas Red. Quadruplex PCR reactions were run in triplicate on a Bio-Rad Laboratories iQ5 using 5′-fluorogenic nuclease TaqMan methodology according to the manufacturer's instructions. Negative controls with no RNA template were included in every analysis, and all samples were normalized with 18S RNA. Results were analyzed using amplification curves and threshold cycles collected from PCR data analysis. PCR primers and probe sequences were as follows: IL-6: forward, 5′-GGTCCAGTTGCCTTCTCC-3′; reverse, 5′-TGTCAATTCGTTCTGAAGAGG-3′; probe, 5′-CGCGATCTGGTGTTGCCTGCTGCCTTCCGATCGCG-3′; G-CFS: forward, 5′-GATGGGTGAGTGTCTTGG-3′; reverse, 5′-ACTGGGTGCCTTTAATCC-3′; probe, 5′-CGCGATCCTGTCACACCAGCCTCCCTCCCGATCGCG-3′; NFκBp65: forward, 5′-GTTCACAGACCTGGCATCC-3′; reverse, 5′-TGTCACTAGGCGAGTTATAGC-3′; probe, 5′-CGCGATCCCACACAACTGAGCCCATGCTGAGATCGCG-3′; NFκBp50: forward, 5′-AATGACAGAGGCGTGTATAAGG-3′; reverse, 5′-GAGCTGCTTGGCGGATTAG-3′; probe, 5′-CGCGATCGCAAATAGGCAAGGTCAGGGTGCAGATCGCG-3′; and 18S RNA: forward, 5′ AGG-AAT-TCC-CAG-TAA-GTG-CG-3′; reverse, 5′-GCCTCA-CTA-AAC-CAT-CCA-A-3′; probe, 5′-TEXASRED-TCCCTGCCCTTTGTACACACCGCC-BHQ2–3′.

NFκB siRNA Transfection. NFκBp65 siRNA from siGENOME SMARTpool (Dharmacon Inc., Lafayette, CO) was transfected into $CD34^{+}$ cells using a Nucleofector II (Amaxa Inc., Gaithersburg, MD) according to the manufacturer's protocol. In brief, 10^{6} $CD34^{+}$ cells were resuspended in 100 μl of human CD34 cell Nucleofector solution (Human $CD34^{+}$ Nucleofector Kit; Amaxa Inc.) with 1.5 μg of

NFκBp65 siRNA-siGENOME SMARTpool and/or 1.5 μg of maxGFP siRNA (positive control provided in the siRNA Test Kit; Amaxa, Inc.). Samples were transferred into an Amaxa-certified cuvette and nucleotransferred with program A-27 using the Nucleofector II. After transfection, cells were immediately transferred into fresh, prewarmed, cytokine-supplemented $CD34^+$ cell culture medium with or without 5-AED. These cells then were cultured in a 37°C incubator until irradiation on the next day (24 h after siRNA transfection). Western blots and colony assays were performed 24 h after IR (48 h after siRNA transfection).

Immunoprecipitation and Immunoblotting. Immunoprecipitation kits from Sigma (St. Louis, MO) were used as follows: 1 to 5 × 10^6 cells from each sample were harvested, washed, and lysed with 0.5 ml of lysis buffer, 1 to 5 μg of purified primary antibody, 1× IP buffer (provided in kit), and protease inhibitor cocktail. Components were added to a spin column and incubated overnight at 4°C with inversion. Precleared protein G beads (20–30 μl) were added to the column and incubated overnight at 4°C. Beads were washed several times at 4°C and the effluent discarded. After the last wash, the supernatant was carefully removed, and 50 μl of 1× Laemmli sample buffer was added to the pellet. After being vortexed and heated to 90 to 100°C for 5 min, samples were spun at 10,000g for 5 min, supernatants were collected for SDS-polyacrylamide gel electrophoresis, and proteins were analyzed by immunoblotting as follows. Protein concentrations were determined using a bicinchoninic acid protein assay kit (Pierce, Rockford, IL). Proteins were separated by SDS-polyacrylamide gel electrophoresis and transferred to nitrocellulose membranes. Membranes were preblocked and probed with primary antibodies (for NFκBp65 and p50, $I\kappa B_\alpha$ and $I\kappa B_\beta$, p53, and loading controls), per the manufacturer's instructions, followed by the appropriate horseradish peroxidase-conjugated secondary antibody (all antibodies were from Santa Cruz Biotechnology, Inc., Santa Cruz, CA). Signal detection used an enhanced chemiluminescence kit (GE Healthcare, Chalfont St. Giles, Buckinghamshire, UK) and Kodak X-ray film (Eastman Kodak, Rochester, NY) (Elagib et al. 2004).

Nuclear Extract Preparation. Nuclear extracts were prepared using a nuclear extraction kit (Panomics Inc., Redwood City, CA) according to the manufacturer's protocol. In brief, cells were washed and resuspended with buffer mix containing 10 mM HEPES, 10 mM KCl, and 10 mM EDTA with dithiothreitol, protease inhibitor cocktail, and IGEPAL. After incubation on ice for 10 min, samples were centrifuged at maximum speed for 3 min at 4°C. The supernatant was discarded and the pellet resuspended in buffer mix containing 20 mM HEPES, 0.4 M NaCl, 1 mM EDTA, and 10% glycerol with protease inhibitor cocktail and dithiothreitol. Eppendorf tubes containing sample were laid horizontally on ice and shaken on a rocking platform at 200 rpm for 2 h. Samples were then centrifuged at maximum speed in an Eppendorf centrifuge for 5 min at 4°C, and supernatants (nuclear extracts) were collected.

Transbinding Assay. An NFκB1 (p50) probe was used with the Transbinding ELISA kit from Panomics, which uses an oligonucleotide-containing NFκB consensus binding site immobilized on a 96-well plate. Activated NFκB from cell nuclear extracts specifically binds to this oligonucleotide. Complexes bound to the oligonucleotide were detected by antibody directed against the p50 subunit and a secondary horseradish peroxidase-conjugated antibody, which was quantified by spectrophotometry. Consensus oligonucleotide was used as a competitor to control for nonspecific binding (Lu and Wahl, 2005).

Cytokine Antibody Array and ELISA for Cytokines in Culture Medium. To determine endogenous hematopoietic factor synthesis in cultures, serum-free culture medium from indicated samples was subjected to cytokine antibody array analysis using the Ray Bio Human Cytokine Antibody Array VII kit (Ray Biotech, Inc. Norcross, GA) according to the manufacturer's instructions. The kit provided antibodies for detection of 60 cytokines, chemokines, growth factors, and soluble receptors of cytokines. In brief, the array membrane coated with cytokine antibodies was first blocked with blocking buffer and then incubated with 1 ml of pooled serum-free culture medium from three individual experiments overnight. After washing and incubation with biotin-conjugated second antibody for 2 h at room temperature, the membranes were washed again and incubated with horseradish peroxidase-conjugated streptavidin. The membrane was developed using enhanced chemiluminescence solution and exposed to X-ray film. Soluble cytokines G-CSF and IL-6 released from serum-free cultured cells were also measured by ELISA kits (R&D Systems, Minneapolis, MN) after normalizing the protein concentration in every sample, according to the company's instructions (Singh et al., 2005).

Modulation of Intercellular Signaling with Neutralizing Antibodies. Neutralization of IL-6 and G-CSF bioactivity was performed as described in the manufacturer's instructions (R&D Systems). In brief, neutralizing antibody (1 μg/ml) or control nonspecific IgG from the same species was added to the culture medium 1 h before cell addition. After this preincubation period, 5 × 10^5 $CD34^+$ cells were added with or without 5-AED administration, and cells were exposed to γ-radiation at the indicated doses. Antibodies were maintained in the cultures after IR. Twenty-four hours after IR, cells were used for colony assays or other indicated assays to determine the effects of IL-6 and G-CSF neutralization.

Statistical Methods. Differences between means were compared by ANOVA and by Student's t tests. $P < 0.05$ was considered statistically significant. Results are presented as means ± S.D.

Results

Effects of 5-AED on Human $CD34^+$ Cell Survival, Differentiation, and Clonogenicity after IR. In pilot studies, 5-AED up to 10 μg/ml had no toxicity, and the optimal dose for enhancing cell survival was 1 μg/ml. The effects of 5-AED were then tested in $CD34^+$ cells adding the steroid before, after, and both before and after IR. The optimal effect was obtained when 5-AED was administered both before and after IR (data not shown). In the next series of experiments, $CD34^+$ cells were cultured with or without 5-AED for 24 h before IR (2, 4, or 6 Gy). After IR, $CD34^+$ cells were immediately transferred to fresh serum-free culture medium supplemented with cytokines and growth factors, with or without 5-AED. Twenty-four hours after IR, apoptotic cell death was dramatically increased ($p < 0.01$, compared with unirradiated controls) and significantly related to radiation dose ($p < 0.05$, 2 Gy compared with 4 Gy, and 4 Gy compared with 6 Gy) as determined by annexin-V and propidium iodide or 7AAD staining using flow cytometry (Fig. 1A). We further analyzed IR-induced apoptosis in both $CD34^+$ and differentiated $CD34^-$ subpopulations in these cultured cells. The percentage of annexin-V and 7AAD-positive apoptotic cells was markedly higher in $CD34^+$ cells than $CD34^-$ differentiated cells at all IR doses (Fig. 1A, $p < 0.01$). Frequencies of Annexin-V- and 7AAD-positive cells decreased with 5-AED in $CD34^+$ cells with 2 and 4 Gy, and in $CD34^-$ cells with 4 and 6 Gy exposures, suggesting that 5-AED protects hematopoietic cells from apoptosis occurring within 24 h after IR (Fig. 1A, $p < 0.05$).

Next, we evaluated the effects of 5-AED on colony-forming potential. Results from one representative experiment (of a total of five) are shown in Fig. 1B. Clonogenic assays starting with 5 × 10^3 cells/dish were plated 24 h after IR. Colony efficiencies for unirradiated $CD34^+$ cells ranged from 15 to 30%, and these efficiencies were not affected by 5-AED. For irradiated cells, BFU-E colonies in 5-AED-treated cultures increased from 163 ± 17 (vehicle-treated) to 418 ± 20 after 2

Gy ($p < 0.01$), and from 59 ± 15 to 118 ± 11 after 4 Gy ($p < 0.05$). CFU-GM colonies in 5-AED-treated cultures rose from 89 ± 6 to 177 ± 13 after 2 Gy ($p < 0.01$) and from 27 ± 3 to 51 ± 3 cells after 4 Gy ($p < 0.01$). 5-AED increased numbers of cells surviving 7 days after IR in these cultures starting with 7.5 × 10^5 cells/culture (Fig. 1C). Seven days after IR, numbers of trypan blue-negative (live) cells from 5-AED-treated cultures were doubled after 2 Gy (from 1.5 ± 0.20 × 10^6 without 5-AED to 3.0 ± 0.29 × 10^6 with 5-AED, $p < 0.01$), and a similar result was obtained after 4 Gy (1.0 ± 0.17 × 10^6 without 5-AED to 1.8 ± 0.23 × 10^6 with 5-AED, $p < 0.01$). In addition, 5-AED administration to irradiated $CD34^+$ cell cultures was associated with a trend toward elevated frequency of $CD11b^+$ cells (granulocytes, monocytes, and NK cells), as determined by flow cytometry 7 to 21 days after IR (Fig. 1, D and E).

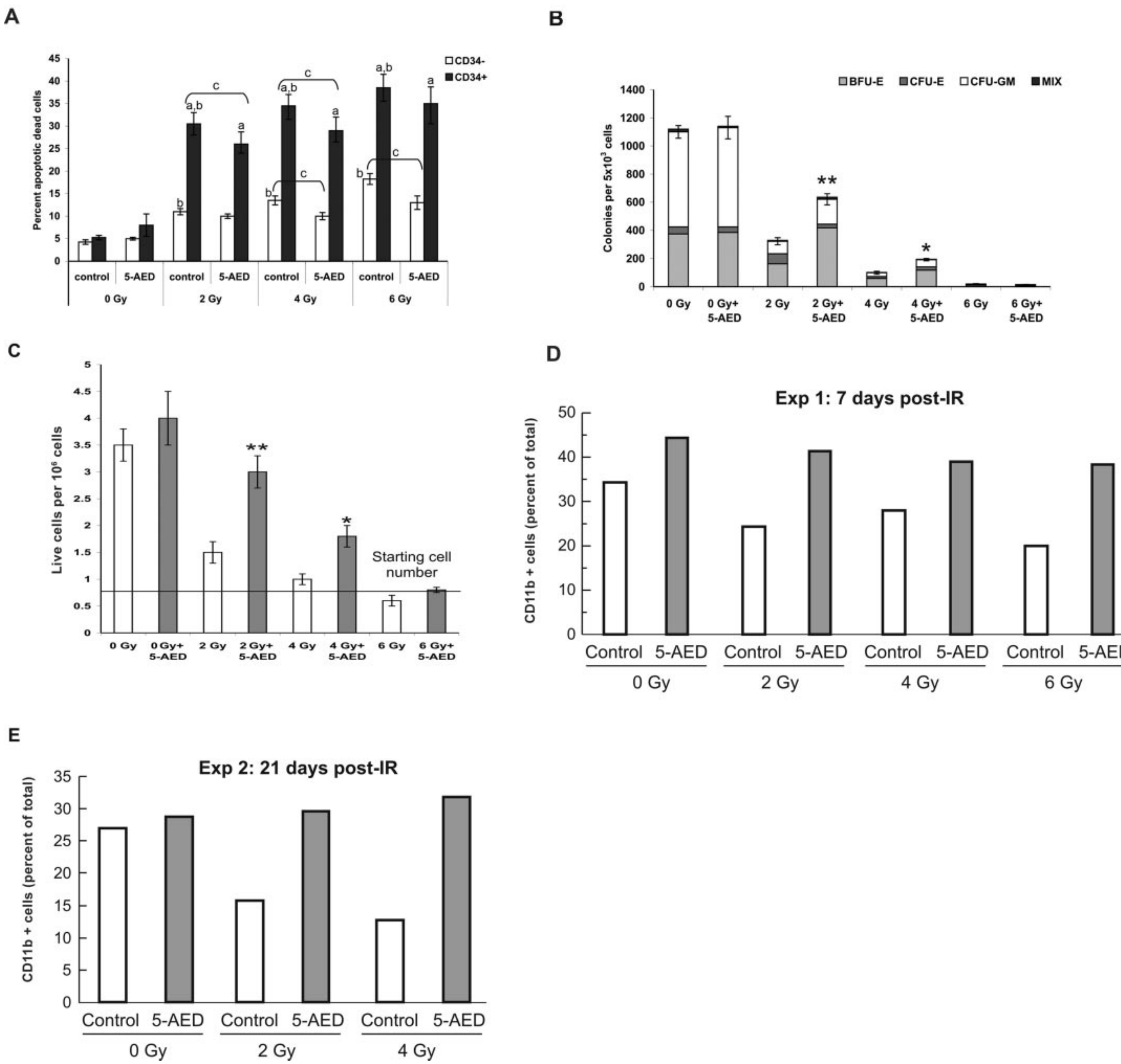

Fig. 1. Effects of IR and 5-AED on human $CD34^+$ cells. A, 24 h after IR or sham IR, apoptotic cell death was determined by annexin-V and 7AAD staining in a total of three experiments. Significant differences: a, $CD34^+$ versus $CD34^-$ cells, ($p < 0.01$); b, radiation dose response ($p < 0.05$, 2 versus 4 Gy and 4 versus 6 Gy); c, 5-AED versus control ($p < 0.05$); means ± S.D. B, cells were plated for clonogenic assays 24 h after IR or sham-IR. 5-AED (1 μg/ml) was added to cultures for a 48-h period starting 24 h before IR or sham-IR. Colonies were counted 14 days later. CFU-MIX, multipotential progenitors; CFU-GM, granulocyte-macrophage progenitors; CFU-E, very early erythroid precursor cells; BFU-E, earliest known erythroid precursor cells. Colony generation in all lineages was inhibited by IR, and this inhibition was ameliorated by 5-AED. Means ± S.D. *, $p < 0.05$; **, $p < 0.01$ (5-AED versus vehicle, for BFU-E and CFU-GM). C, in separate cells from the same experiment, 5-AED enhanced survival (trypan blue assay) of $CD34^+$ cells 7 days after IR. The starting cell number was 7.5 × 10^5 per culture as shown by the horizontal line. Means ± S.D. **, $p < 0.01$ (5-AED versus vehicle). Results (B and C) were from one representative experiment of a total of five independent experiments, and each experiment was performed in triplicate. D and E, 5-AED administration was associated with a trend toward elevated frequency of $CD11b^+$ cells as determined by flow cytometry from two independent experiments 7 (D) and 21 (E) days after IR.

Role of NFκB in 5-AED Effects. Because of the limited number of CD34$^+$ cells after IR, we evaluated IR and 5-AED-mediated NFκB activation in CD34$^+$ cells using a DNA-binding assay. The transbinding NFκB assay is more sensitive than electrophoretic mobility shift assay, is comparable in specificity, and requires fewer cells per sample (Lu and Wahl, 2005). Results from nuclear extracts obtained 24 h after IR (Fig. 2A) demonstrated that 5-AED but not IR stimulated NFκB activity in CD34$^+$ cultures ($p < 0.01$ at 0 and 2 Gy, $p < 0.05$ at 4 Gy). Unirradiated, untreated samples (Fig. 2A, 0 Gy) did not display detectable levels of NFκB activity in this assay (compare with 5-AED + competitor probe).

To characterize the activation of NFκB as a transcriptional activator in CD34$^+$ cells and to verify that 5-AED-stimulated NFκB activation is associated with its radiation countermeasure function, we used peptide aldehyde MG132, a potent proteasome inhibitor that prevents degradation of the regulatory molecule IκB (Guzman et al., 2001; Lin and Kobayashi, 2003). Previous reports indicated 1.0 μM MG132 has no toxicity in unstimulated normal human CD34$^+$ cells (Guzman et al., 2001). Therefore, doses of MG132 from 0.1 to 0.5 μM were added 1 h before IR to CD34$^+$ cultures with and without 5-AED administration. As shown in Fig. 2B, NFκBp65 (RelA) subunit expression was detected by immunoblotting in nuclear extracts from unirradiated and irradiated samples. As described under *Materials and Methods*, all CD34$^+$ cells were cultured in the presence of SCF, rh flt-3 ligand, and IL-3 for 72 h before IR, which might explain the

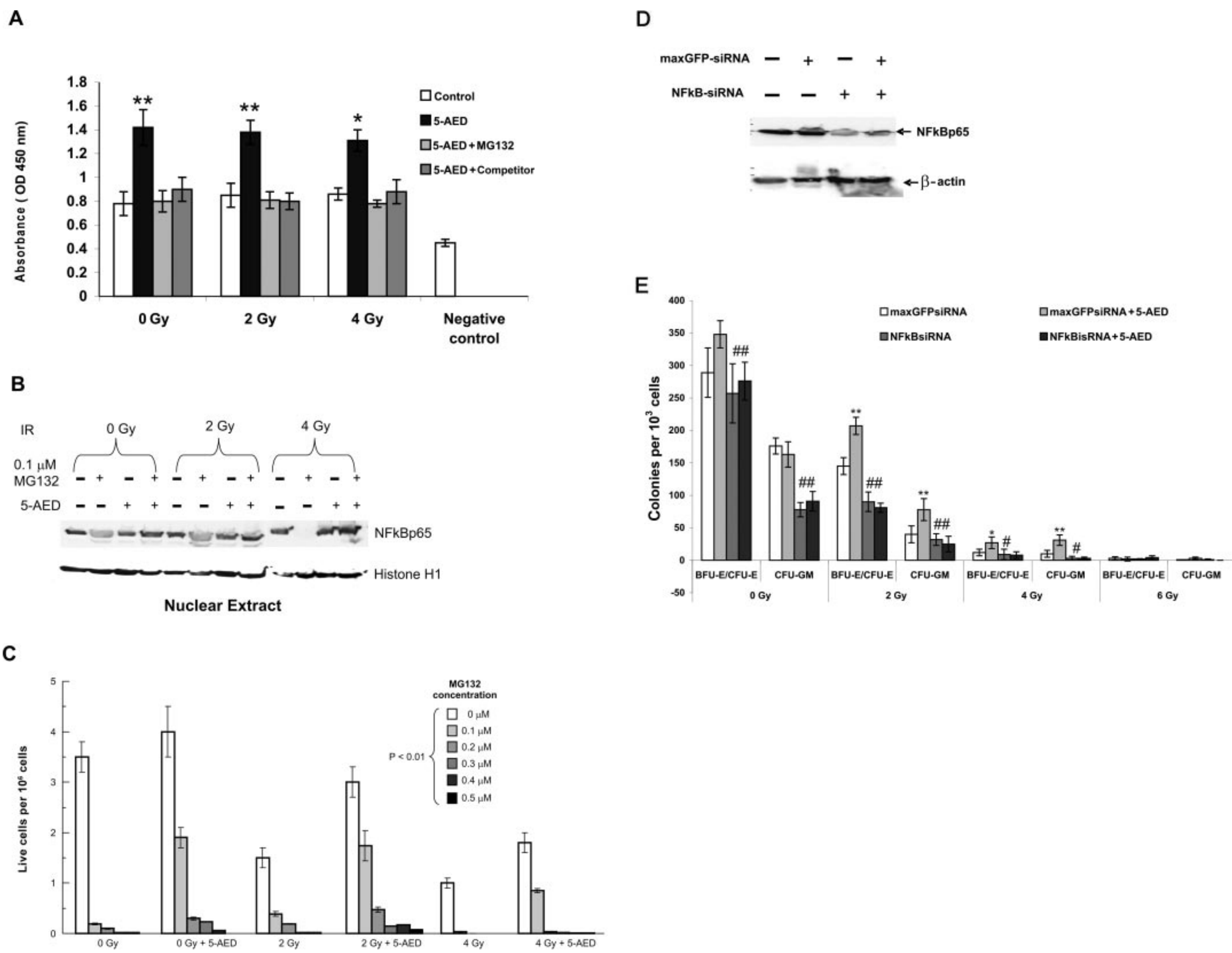

Fig. 2. 5-AED but not IR stimulated NFκB activation in CD34$^+$ cells. A, activation of the antiapoptotic transcription factor NFκB was analyzed with a DNA-binding ELISA assay as described under *Materials and Methods*. 5-AED (1 μg/ml) was added to cultures for a 48-h period starting 24 h before IR. Background levels for the assay are shown by the "5-AED + competitor" values. Results were from a total of three experiments, and each experiment was performed in triplicate. Means ± S.D. *, $p < 0.05$; **, $p < 0.01$ (5-AED versus vehicle control) B, Western blot shows MG132 treatment (1 h, 0.1 μM) down-regulated NFκBp65 levels in CD34$^+$ cell nuclear extracts, suggesting that NFκB relocation from cytoplasm to nucleus was inhibited. 5-AED blocked this MG132 effect. C, different doses of MG132 from 0.1 to 0.5 μM were added to CD34$^+$ cultures 1 h before IR. 5-AED (1 μg/ml) or vehicle was added to cultures for a 48-h period starting 24 h before IR. Survival of CD34$^+$ cells 7 days after IR was assayed using trypan blue. MG132 concentrations are shown in the legend. MG132 treatment at every concentration caused significant decreases in numbers of surviving cells ($p < 0.01$). The beneficial effects of 5-AED were abrogated by all concentrations of MG132. Data from a total of three experiments. D, Western blot shows NFκBp65 and β-actin (loading control) expression in control, NFκBp65-siRNA-transfected, maxGFP-siRNA-transfected, and NFκBp65 + maxGFP-siRNA-cotransfected samples. E, cells were plated for clonogenic assays 48 h after siRNA transfection and 24 h after IR. 5-AED (1 μg/ml) was added to cultures for a 48-h period starting 24 h before IR. Means ± S.D. *, $p < 0.05$; **, $p < 0.01$ (5-AED treatment versus control); #, $p < 0.05$; ##, $p < 0.01$ (NFκBp65-siRNA transfected cells versus maxGFP-siRNA transfected cells, with or without 5-AED treatment).

baseline expression of NFκBp65. IR (2 or 4 Gy) had no effect on NFκBp65 levels. In the absence of 5-AED, MG132 treatment at concentrations as low as 0.1 μM dramatically down-regulated NFκBp65 expression, suggesting that NFκB translocation from cytoplasm to nucleus was inhibited by MG132 (Fig. 2B). Addition of 5-AED did not up-regulate NFκBp65 expression. However, it blocked NFκBp65 down-regulation in MG132-treated nuclear extracts. Separate samples from the same experiment were cultured for 7 days after IR, and trypan blue-negative cells were counted. Figure 2C shows that MG132 inhibited cell survival and expansion in a dose-dependent fashion. The effects of 5-AED on survival of irradiated $CD34^+$ cells were abrogated by even the lowest dose of MG132. Consistent with results from the immunoblotting assay, 5-AED partially protected cells from the lower dose (0.1 μM) of MG132, whereas 0.5 μM MG132 completely inhibited $CD34^+$ cell growth.

MG132 is a general proteasome inhibitor that affects a wide variety of cellular processes. Therefore, we also evaluated the effect of a more specific NFκB inhibitor. NFκB siRNA was transfected into $CD34^+$ cells before 5-AED administration and IR using Nucleofector technology as described under *Materials and Methods*. NFκB siGENOME SMARTpool (Dharmacon) contains a mixture of four siRNAs targeting one human NFκBp65 gene, which silences gene expression at the mRNA level by at least 75%. Western blots and colony assays were performed 48 h after NFκBp65 siRNA and/or positive control siRNA (maxGFP siRNA) transfection with or without 5-AED administration and 24 h after irradiation. Results from Western blot (Fig. 2D) showed NFκB protein levels markedly decreased after NFκBp65 siRNA transfection. In contrast, control siRNA-transfected cells expressed NFκB at the same level as nontransfected samples. Colony efficiencies were dramatically inhibited by NFκB gene knockdown in both erythroid (BFU-E and CFU-E) and myeloid (CFU-GM) lineages compared with control siRNA-transfected samples (Fig. 2E). The effect of 5-AED induced clonogenicity at different doses of IR was completely blocked in NFκB siRNA-transfected samples (Fig. 2E).

Ionizing Radiation but Not 5-AED Induced $I\kappa B_\beta$ Release from NFκB/IκB Complexes. NFκB is normally sequestered in the cytoplasm of unstimulated cells in a complex with IκB. NFκB can be rapidly released by degradation of IκB and can enter the nucleus without a requirement for de novo protein synthesis (Thompson et al., 1995; Joyce et al., 2001). The overall activation of NFκB consists of two overlapping phases, a transient phase mediated by $I\kappa B_\alpha$ degradation, and a persistent phase mediated through $I\kappa B_\beta$ degradation. Although our data showed NFκBp65 expression in irradiated cell nuclear extracts, there was no evidence of IR-induced NFκB activation in these cultured $CD34^+$ cells as determined by the DNA-binding assay. Because of the relatively low level of IκBs in $CD34^+$ cells, IκB expression and phosphorylation were undetectable in total cell lysates by Western blot. Therefore, to address the question of whether IR and/or 5-AED induces IκB release from NFκB/IκB complexes, immunoprecipitation (IP) was used to evaluate NFκB/IκB protein interaction. Cell lysates were subjected to IP with an NFκBp65 antibody. After SDS-gel separation, protein levels were assessed by immunoblotting using antibodies to NFκBp65, NFκBp50, $I\kappa B_\alpha$, and $I\kappa B_\beta$. Figure 3 shows that, 4 h after IR, $I\kappa B_\alpha$ signal was not detectable in any sample, presumably caused by baseline activation of the NFκB pathway by the cytokines added to the culture medium. $I\kappa B_\beta$ was detectable in NFκB/IκB complexes but was attenuated by IR in a dose-dependent fashion. Compared with unirradiated cells, $I\kappa B_\beta$ present in NFκB/IκB complexes was similar after 2 Gy, lower after 4 Gy, and undetectable after 6 Gy (Fig. 3). Twenty-four hours after IR, levels of $I\kappa B_\beta$ were barely detectable in any sample (data not shown). 5-AED did not change patterns of $I\kappa B_\beta$ disappearance from NFκB/IκB complexes.

NFκB Gene and Protein Expression in Cultured $CD34^+$ Cells with and without IR and 5-AED. Because 5-AED significantly stimulated NFκB activity in $CD34^+$ cells, but we did not detect an effect of 5-AED on NFκB translocation or IκB degradation, we decided to assess 5-AED-induced NFκB expression. First, NFκB gene expression was measured using multiplex QRT-PCR, which allowed us to assay 18S rRNA and NFκB subunits p65 and p50 simultaneously in the same sample. Gene expression was expressed as a relative quantity normalized to 18S rRNA. Figure 4A shows that NFκB gene expression was unchanged 4 h after IR or sham-IR, with or without 5-AED treatment, whereas 5-AED enhanced NFκBp65 mRNA levels 5-fold 24 h after sham-IR and 6-fold 24 h after 4 Gy, compared with vehicle-treated cultures. Subunit NFκBp50 mRNA expression was also induced by 5-AED (to three times control levels) 24 h after 4 Gy IR. NFκBp50 gene expression was not increased 24 h after IR alone (Fig. 4A).

Second, we used Western blots to determine NFκBp65 and NFκBp50 protein levels in whole-cell lysates from cultured $CD34^+$ cells. NFκBp65 levels displayed no differences between treatments (Fig. 4B). NFκBp50 antibody was then used on the same membranes, after anti-NFκBp65 antibody was stripped. IR caused protein degradation and low molecular mass fragments in a dose-dependent manner (Fig. 4B). IR-induced NFκBp50 damage could directly affect NFκB dimerization, DNA binding, and transcriptional activity. Stability of the Rel homology domain is critical for NFκBp50 generation (Lin et al., 2000; Lin and Kobayashi, 2003; Carlsen et al., 2004) The Rel homology domain consists of two structurally similar subdomains, sd1 and sd2, linked by a short loop. In Fig. 4B, small fragments with the molecular mass of sd1 (Lin and Kobayashi, 2003) are evident after IR at doses of 4 and 6 Gy. Addition of 5-AED before or after IR decreased the appearance of this fragment, and the fragment

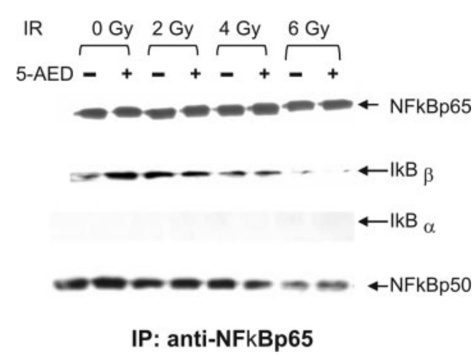

Fig. 3. IR but not 5-AED induced $I\kappa B_\beta$ release from NFκB/IκB complexes. $CD34^+$ cell lysates collected at 4 h after IR with or without 5-AED were subjected to immunoprecipitation using an NFκBp65 antibody. After SDS-gel separation, proteins were analyzed by immunoblotting using anti-NFκBp65, NFκBp50, $I\kappa B_\alpha$, and $I\kappa B_\beta$ antibodies.

was undetectable when 5-AED was administered both before and after IR. These effects of 5-AED were consistent in all experiments (n = 9).

G-CSF and IL-6 Production Induced by 5-AED. Our previous in vivo studies demonstrated that 5-AED induced the hematopoietic growth factors IL-6 and G-CSF in mice (Singh et al., 2005). To test our hypothesis that 5-AED acts via initiation of a cytokine cascade in hematopoietic cells, secreted cytokines and chemokines were assayed in serum-free medium from CD34$^+$ cells 24 h after IR with or without 5-AED, using a cytokine antibody array. In Fig. 5A, results from three individual experiments' samples pooled demonstrated significant G-CSF elevations after 4 Gy, with and without 5-AED. Next, we quantitated IL-6 and G-CSF expression at the mRNA and protein levels using QRT-PCR and ELISA. 5-AED elevated IL-6 mRNA levels 2-fold in CD34$^+$ cells without IR and 10-fold 4 h after 4 Gy compared with vehicle-treated cultures (Fig. 5B). Twenty-four hours after sham-irradiation or irradiation, 5-AED-induced IL-6 mRNA levels were still higher than in vehicle-treated cultures (Fig. 5B). The G-CSF mRNA level increased 17-fold in 5-AED-treated cultures 4 h after 4 Gy (Fig. 5C) and returned to baseline levels 24 h after IR (data not shown). Consistent with these results, 5-AED elevated IL-6 secretion (Fig. 5D) from CD34$^+$ cell cultures 6-fold 24 h after 4 Gy and 10-fold after 6 Gy measured by ELISA. After 4 days in culture, IL-6 protein levels were elevated by 5-AED treatment (1 μg/ml) in both unirradiated and irradiated cultures. Observations of G-CSF secretion from CD34$^+$ cell cultures were consistent with the cytokine antibody array results. 5-AED elevated G-CSF levels after 0 Gy (from 0.6 ± 0.31 vehicle control to 1.2 ± 0.4 pg/ml), 2 Gy (from 1.8 ± 0.22 to 2.7 ± 0.25 pg/ml, $p < 0.05$), and 4 Gy (from 0.96 ± 0.25 to 2.0 ± 0.2 pg/ml, $p < 0.05$) (Fig. 5E). Irradiation alone (2 Gy) induced an increase in G-CSF protein level (Fig. 5E).

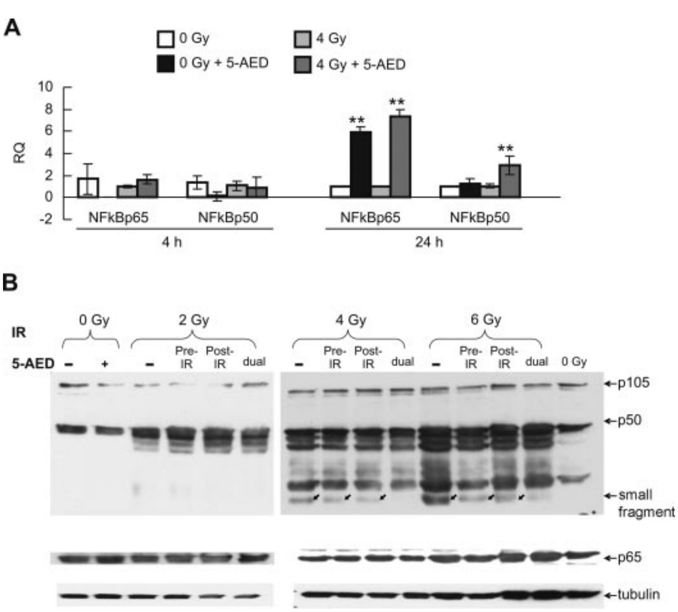

Fig. 4. Effect of 5-AED on NFκB expression in CD34$^+$ cells. A, NFκB gene expression was measured using multiplex QRT-PCR, and 18S rRNA as a control to calculate the relative quantity of gene expression 4 and 24 h after 0 or 4 Gy IR with and without 5-AED administration. Means ± S.D. *, $p < 0.05$; **, $p < 0.01$ (5-AED versus vehicle). B, Western blot determination of NFκBp65 and NFκBp50 subunit expression in whole-cell lysates. NFκBp65 levels were similar after all treatments. Immunoblot using anti-NFκBp50 antibody on the same membrane after anti-NFκBp65 antibody was stripped showed NFκBp50 protein degradation and a low molecular mass fragment (27–32 kDa, tentatively identified as "small fragment", small arrows on gels) after IR (4 and 6 Gy). Addition of 5-AED before or after IR decreased levels of the low molecular mass fragment, and when 5-AED was administered both before and after IR ("dual"), the small fragment disappeared.

Levels of IL-6 and G-CSF were measured 48 h after NFκB inhibitor MG132 (0.1 μM) addition to CD34$^+$ cells with and without 5-AED treatment and IR. Figure 5F shows that MG132 up-regulated IL-6 release from irradiated cells ($p < 0.01$), and this effect of MG132 was correlated with radiation dose. In contrast, 5-AED-induced G-CSF secretion was blocked by MG132 administration, as shown in Fig. 5G. After both 2 and 4 Gy, G-CSF levels were significantly greater than vehicle control levels after 5-AED alone but not after 5-AED plus MG132 (Fig. 5G).

5-AED Effects Mediated by G-CSF, Not IL-6 or p53. To evaluate the potential role of G-CSF and IL-6 in the effects of 5-AED, neutralizing antibodies were used. Antihuman G-CSF or antihuman IL-6 antibody (1 μg/ml) was added to culture medium 1 h before 5-AED administration and 25 h before IR and maintained in the cultures after IR with or without 5-AED addition. As shown in Fig. 6, A and B, the addition of anti-G-CSF antibody inhibited colony formation in irradiated cells and impaired the effect of 5-AED on progenitor cell survival. Anti-IL-6 antibody did not inhibit colony efficiency: 5-AED administration significantly increased colony numbers in irradiated CD34$^+$ cells both with and without IL-6 neutralization (Fig. 6C).

The tumor suppressor gene p53 plays an important role in apoptosis and cell death (Fei and El-Deiry, 2003). The p53 protein is tightly regulated and remains at low levels in unstressed cells, but is rapidly activated (stabilized) by various types of cellular stresses, including IR. To test whether the effects of 5-AED in irradiated CD34$^+$ cells correlated with p53 signaling, p53 protein expression was determined by Western blot (Fig. 6D). Expression of p53 in unirradiated cells was undetectable. Four hours after IR (4 Gy), p53 was clearly induced, and levels had declined by 24 h after IR but were still present. 5-AED had no effect on p53 levels.

Discussion

We showed previously that 5-AED (HE2100, the active principal ingredient of NEUMUNE) induces production of G-CSF (Singh et al., 2005), stimulates hematopoiesis (Whitnall et al., 2000; Stickney et al., 2006, 2007), and enhances survival in mice (Whitnall et al., 2000) and monkeys (Stickney et al., 2007) exposed to whole-body γ-IR. However, the intracellular signaling pathways that mediate these beneficial effects of 5-AED were unknown. Moreover, it was not known whether 5-AED can act directly on hematopoietic tissue or whether its actions were dependent on indirect effects on other tissues. The present results demonstrate that 5-AED acts directly on cells from hematopoietic tissue.

In this report, we used in vitro approaches to evaluate the radiation countermeasure effects of 5-AED in primary human hematopoietic CD34$^+$ cells. Our results showed that 5-AED improved CD34$^+$ cell survival, proliferation, and differentiation into functional hematopoietic lineages after IR. 5-AED induced NFκB activation in cultured CD34$^+$ cells, as confirmed using a DNA-binding assay. In contrast, γ-radiation did not stimulate the activity of NFκB in these cells. To characterize the activation of NFκB as a transcriptional activator in $CD34^+$ cells and to verify that 5-AED-stimulated NFκB activation is associated with its radiation countermeasure function, a proteasome inhibitor, MG132, was used to inhibit NFκB activation. Our results indicate that 5-AED-induced cell survival of irradiated $CD34^+$ cells is inhibited by MG132. However, as noted, MG132 affects a wide variety of cellular processes. Therefore, we evaluated the effect of 5-AED in NFκBp65 gene knockdown cells using colony-forming assays. NFκBp65 siRNA transfection significantly inhibited NFκBp65 protein expression and clonogenicity of $CD34^+$ cells and completely blocked the effect of 5-AED on clonogenic cell survival after irradiation. These results support our hypothesis that 5-AED promotes survival of γ-irradiated human hematopoietic progenitors through induction of NFκB activation.

In the present study, IR-induced IκB release from NFκB/IκB complexes was confirmed by IP. $I\kappa B_\beta$ but not $I\kappa B_\alpha$ levels in NFκB/IκB complexes were attenuated by radiation in a dose-dependent fashion, suggesting that this persistent phase regulator of NFκB activation played a key role in radiation-induced NFκB translocation to the nucleus of $CD34^+$ cells. The major difference between the $I\kappa B_\alpha$ and $I\kappa B_\beta$ isoforms lies in their responses to different inducers of NFκB activity and their different mechanisms of NFκB regulation (Thompson et al., 1995; Malek et al., 2001; Russell and Tofilon, 2002). A previous report (Basu et al., 1998) demonstrated that IR, but not tumor necrosis factor-α, induced DNA-dependent protein kinase (DNA-PK) activity. $I\kappa B_\alpha$ was a poor substrate, whereas $I\kappa B_\beta$ was strongly phosphorylated by DNA-PK in two distinct regions after IR-induced DNA damage. Therefore, activation of NFκB by DNA-PK after DNA damage may proceed through direct phosphorylation of $I\kappa B_\beta$. Those results indicated that IR induced the activity of NFκB beginning 2 to 4 h after exposure. In contrast, tumor necrosis factor-α-mediated activation of NFκB occurs with peak activation at 30 min (Russell and Tofilon, 2002). These observations were consistent with our observations, in which $I\kappa B_\beta$ was released from NFκB/IκB complexes within 4 h after IR. We were surprised to find that although IR induced $I\kappa B_\beta$ degradation and release from NFκB/IκB complexes, it did not induce NFκB activation (DNA binding). In contrast, 5-AED

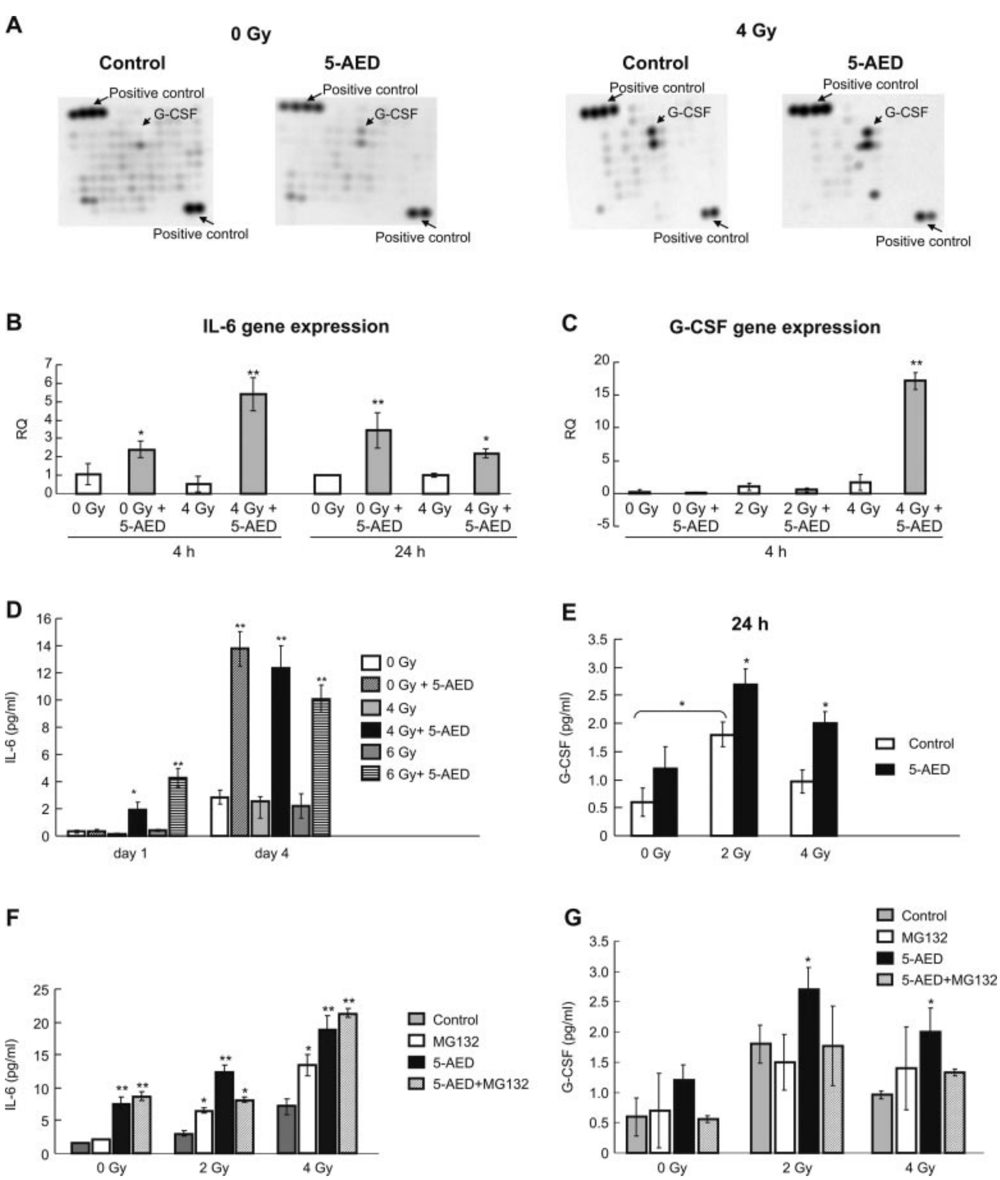

Fig. 5. Effects of 5-AED on IL-6 and G-CSF expression in irradiated $CD34^+$ cells. A, a cytokine antibody array was used with pooled serum-free culture medium from $CD34^+$ cultures with and without IR and 5-AED. B and C, 5-AED (1 μg/ml) was added to cultures for a 48-h period starting 24 h before IR. IL-6 (B) and G-CSF (C) gene expression was determined by QRT-PCR. D and E, 5-AED stimulated IL-6 (D) and G-CSF (E) secretion as determined by ELISA. Means ± S.D. *, $p < 0.05$; **, $p < 0.01$ (5-AED versus vehicle, and unirradiated versus 2 Gy for G-CSF level). F and G, levels of IL-6 (F) and G-CSF (G) were measured 48 h after IR. The NFκB inhibitor MG132 (0.1 μM) was added 1 h before IR. 5-AED or vehicle (1 μg/ml) was added for a 48-h period starting 24 h before IR. Means ± S.D. *, $p < 0.05$; **, $p < 0.01$ (versus vehicle-treated control)

did not increase NFκB translocation and IκB release in irradiated cells, but it significantly stimulated NFκB activity. Therefore, 5-AED-mediated NFκB activation in $CD34^+$ cells was not through acceleration of IκB phosphorylation and ubiquitination. Our results indicate that NFκB activation may involve instead up-regulation of NFκB expression and stabilization of the p50 subunit.

To investigate the mechanisms of 5-AED-induced NFκB activation, we assessed NFκB expression. Evidence of 5-AED-induced NFκBp65 mRNA expression was obtained 24 h after IR or sham-IR, whereas NFκBp50 mRNA expression was enhanced by 5-AED only in irradiated cells. Protein levels of NFκBp65 showed the same expression patterns in all samples. For NFκBp50, the small molecular mass fragment appearing in irradiated samples needs further definition, but the disappearance of this fragment in 5-AED-treated cultures was consistently observed in all experiments. Functional NFκBp65/p50 dimers bind specific κB sites on target DNA sequences. The three-dimensional structure of a p65/p50 dimer bound to DNA reveals that NFκB proteins adopt a specific and unique conformation to recognize DNA using loops from both subunits and not α helixes like other transcription factors (Jacobs and Harrison, 1998; Magné et al., 2006). Each subunit contacts one half of the specific binding sites on DNA; therefore, activity of NFκB needs both p65 and p50 subunits. We propose that NFκBp50 degradation after IR may be partly responsible for the radiation sensitivity of $CD34^+$ cells, compared with tumor cells. Although IR induced IκB release from NFκB complexes, resulting in NFκB translocation into the nucleus, IR-induced NFκBp50 protein degradation may block NFκB activation in $CD34^+$ cells. We could not observe an IR-induced decrease in NFκB activity, because unirradiated, untreated samples did not display detectable levels of NFκB activity. 5-AED stimulates NFκB gene expression and stabilizes the p50 subunit, resulting in NFκB activation, which protects $CD34^+$ cells from IR injury.

In this study, 5-AED-induced IL-6 and G-CSF production was evident at the mRNA and protein levels after IR. The results of our G-CSF neutralization experiments showed that 5-AED-induced G-CSF release significantly promoted survival of hematopoietic progenitor cells. The IL-6 and G-CSF gene promoters have binding sites for multiple transcription factors including activator protein-1, NFκB, cAMP response element-binding protein, and CCAAT enhancer binding proteins. Previous reports indicated that the NFκB-binding site is crucial for the activation of the IL-6 and G-CSF promoters (Dunn et al., 1994; Vanden Berghe et al., 2000). Therefore, G-CSF and IL-6 function in response to many stress stimuli, including IR, most likely is under NFκB regulation. In the present study, levels of G-CSF were inhibited by MG132. The results suggest that G-CSF is a survival factor downstream of NFκB activation induced by 5-AED. We were surprised to find that our data showed that 5-AED-induced IL-6 expres-

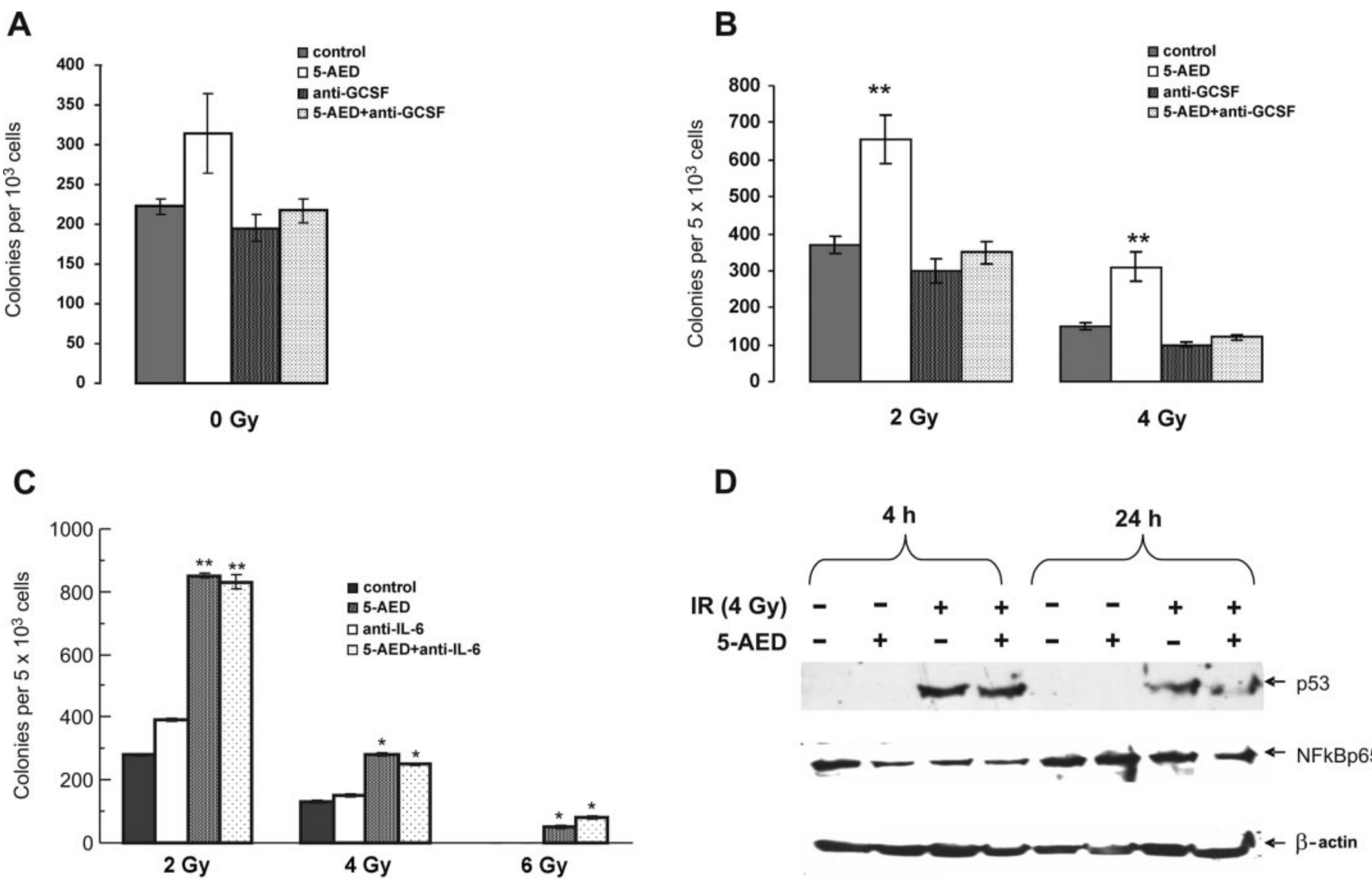

Fig. 6. The beneficial effects of 5-AED are dependent on G-CSF but not IL-6 or changes in p53 levels. G-CSF (A and B) or IL-6 (C) neutralizing antibody (1 μg/ml) or nonspecific IgG from the same species was added to the culture medium 1 h before cell addition. After this preincubation period, 5×10^5 $CD34^+$ cells were added with or without 5-AED administration, and cells were irradiated 24 h later. 24 h after IR, cells were plated for colony assays. Means ± S.D. *, $p < 0.05$; **, $p < 0.01$ (5-AED versus vehicle). D, p53 protein levels were determined by Western blot. p53 in unirradiated cells was undetectable. In contrast, IR (4 Gy) dramatically induced p53 expression in $CD34^+$ cell cultures after 4 and 24 h. 5-AED had no effect on p53 levels. NFκBp65 and β-actin protein levels (used as controls) were assayed on the same membrane after p53 antibody was stripped.

sion is not regulated by NFκB. Other studies have also shown increased IL-6 production after MG132 administration (Pritts et al., 2002) and in NFκB1 (p50) knockout mice (Zhou et al., 2001). Neutralizing IL-6 with an antibody did not reduce clonogenicity in CD34$^+$ cells and did not block the effects of 5-AED, indicating that the radiation countermeasure effects of 5-AED in this experimental system are not dependent on IL-6. In addition, although IR dramatically induced p53 expression in CD34$^+$ cells, 5-AED had no effect on p53 levels, suggesting that the effects of 5-AED on CD34$^+$ cells are p53-independent. In summary, our results demonstrate that IR stimulated IκB release from NFκB/IκB complexes in CD34$^+$ cells. However, we observed IR-induced NFκB1 (p50) degradation in CD34$^+$ cells, which may explain their high radiosensitivity. 5-AED rescued CD34$^+$ progenitor cells from IR through stabilizing NFκB1 and stimulating NFκB expression and activation, resulting in downstream production of the hematopoietic survival factor G-CSF.

In the present report, 5-AED protected CD34$^+$ cells from 4 Gy IR. The moderate dose range (1–7 Gy in humans) poses a risk of damage to the hematopoietic system and results in mortality caused by opportunistic infection and hemorrhage (Coleman et al., 2004). We hope that 5-AED will be useful at doses higher than 4 Gy, although significant decreases in mortality would be expected even if that were the limit, because the LD_{50} in humans is approximately 3.5 Gy. In addition, although we demonstrated direct effects of 5-AED on progenitor cells here, the beneficial effects of 5-AED in vivo may partially be mediated indirectly (i.e., via actions on other cell types or other tissues). We are presently investigating these issues.

References

Basu S, Rosenzweig KR, Youmell M, and Price BD (1998) The DNA-dependent protein kinase participates in the activation of NF kappa B following DNA damage. *Biochem Biophys Res Commun* **247:**79–83.

Besançon F, Atfi A, Gespach C, Cayre YE, and Bourgeade MF (1998) Evidence for a role of NF-κB in the survival of hematopoietic cells mediated by interleukin 3 and the oncogenic TEL/platelet-derived growth factor receptor β fusion protein. *Proc Natl Acad Sci U S A* **95:**8081–8086.

Braun T, Carvalho G, Coquelle A, Vozenin MC, Lepelley P, Hirsch F, Kiladjian JJ, Ribrag V, Fenaux P, and Kroemer G (2006) NF-kappaB constitutes a potential therapeutic target in high-risk myelodysplastic syndrome. *Blood* **107:**1156–1165.

Carlsen H, Alexander G, Austenaa LM, Ebihara K, and Blomhoff R (2004) Molecular imaging of the transcription factor NF-kappaB, a primary regulator of stress response. *Mutat Res* **551:**199–211.

Coleman CN, Stone HB, Moulder JE, and Pellmar TC (2004) Medicine. Modulation of radiation injury. *Science* **304:**693–694.

Dooley DC, Oppenlander BK, and Xiao M (2004) Analysis of primitive CD34- and CD34+ hematopoietic cells from adults: gain and loss of CD34 antigen by undifferentiated cells are closely linked to proliferative status in culture. *Stem Cells* **22:**556–569.

Dunn SM, Coles LS, Lang RK, Gerondakis S, Vadas MA, and Shannon MF (1994) Requirement for nuclear factor (NF)-kappa B p65 and NF-interleukin-6 binding elements in the tumor necrosis factor response region of the granulocyte colony-stimulating factor promoter. *Blood* **83:**2469–2479.

Elagib KE, Xiao M, Hussaini IM, Delehanty LL, Palmer LA, Racke FK, Birrer MJ, Shanmugasundaram G, McDevitt MA, and Goldfarb AN (2004) Jun blockade of erythropoiesis: role for repression of GATA-1 by HERP2. *Mol Cell Biol* **24:**7779–7794.

Fei P and El-Deiry WS (2003) P53 and radiation responses. *Oncogene* **22:**5774–5783.

Granelli-Piperno A, Pope M, Inaba K, and Steinman RM (1995) Coexpression of NF-kappa B/Rel and Sp1 transcription factors in human immunodeficiency virus 1-induced, dendritic cell-T-cell syncytia. *Proc Natl Acad Sci U S A* **92:**10944–10948.

Griffin GE, Leung K, Folks TM, Kunkel S, and Nabel GJ (1989) Activation of HIV gene expression during monocyte differentiation by induction of NF-kappa B. *Nature* **339:**70–73.

Guzman ML, Neering SJ, Upchurch D, Grimes B, Howard DS, Rizzieri DA, Luger SM, and Jordan CT (2001) Nuclear factor-kappaB is constitutively activated in primitive human acute myelogenous leukemia cells. *Blood* **98:**2301–2307.

Jacobs MD and Harrison SC (1998) Structure of an IkappaBalpha/NF-kappaB complex. *Cell* **95:**749–758.

Joyce D, Albanese C, Steer J, Fu M, Bouzahzah B, and Pestell RG (2001) NF-kappaB and cell-cycle regulation: the cyclin connection. *Cytokine Growth Factor Rev* **12:**73–90.

Karin M and Ben-Neriah Y (2000) Phosphorylation meets ubiquitination: the control of NF-kappaB activity. *Annu Rev Immunol* **18:**621–663.

Kim BY, Kim KA, Kwon O, Kim SO, Kim MS, Kim BS, Oh WK, Kim GD, Jung M, and Ahn JS (2005) NF-kappaB inhibition radiosensitizes Ki-Ras-transformed cells to ionizing radiation. *Carcinogenesis* **26:**1395–1403.

Lin L, DeMartino GN, and Greene WC (2000) Cotranslational dimerization of the Rel homology domain of NF-kappaB1 generates p50–p105 heterodimers and is required for effective p50 production. *EMBO J* **19:**4712–4722.

Lin L and Kobayashi M (2003) Stability of the Rel homology domain is critical for generation of NF-kappa B p50 subunit. *J Biol Chem* **278:**31479–31485.

Lu Y and Wahl LM (2005) Oxidative stress augments the production of matrix metalloproteinase-1, cyclooxygenase-2, and prostaglandin E2 through enhancement of NF-kappa B activity in lipopolysaccharide-activated human primary monocytes. *J Immunol* **175:**5423–5429.

Luo JL, Kamata H, and Karin M (2005) IKK/NF-kappaB signaling: balancing life and death—a new approach to cancer therapy. *J Clin Invest* **115:**2625–2632.

Magné N, Toillon RA, Bottero V, Didelot C, Houtte PV, Gerard JP, and Peyron JF (2006) NF-kappaB modulation and ionizing radiation: mechanisms and future directions for cancer treatment. *Cancer Lett* **231:**158–168.

Malek S, Chen Y, Huxford T, and Ghosh G (2001) IκBβ, but not IκBα, functions as a classical cytoplasmic inhibitor of NF-κB dimers by masking both NF-κB nuclear localization sequences in resting cells. *J Biol Chem* **276:**45225–45235.

McDonald PP, Bald A, and Cassatella MA (1997) Activation of the NF-kappaB pathway by inflammatory stimuli in human neutrophils. *Blood* **89:**3421–3433.

Pahl HL (1999) Activators and target genes of Rel/NF-κB transcription factors. *Oncogene* **18:**6853–6866.

Pritts TA, Hungness ES, Hershko DD, Robb BW, Sun X, Luo GJ, Fischer JE, Wong HR, and Hasselgren PO (2002) Proteasome inhibitors induce heat shock response and increase IL-6 expression in human intestinal epithelial cells. *Am J Physiol Regul Integr Comp Physiol* **282:**R1016–1026.

Pyatt DW, Stillman WS, Yang Y, Gross S, Zheng JH, and Irons RD (1999) An essential role for NF-kappaB in human CD34$^+$ bone marrow cell survival. *Blood* **93:**3302–3308.

Romano MF, Lamberti A, Bisogni R, Garbi C, Pagnano AM, Auletta P, Tassone P, Turco MC, and Venuta S (1999) Amifostine inhibits hematopoietic progenitor cell apoptosis by activating NF-kappaB/Rel transcription factors. *Blood* **94:**4060–4066.

Romano MF, Petrella A, Bisogni R, Turco MC, and Venuta S (2003) Effect of NF-kappaB/Rel inhibition on spontaneous vs chemotherapy-induced apoptosis in AML and normal cord blood CD34+ cells. *Leukemia* **17:**1190–1192.

Russell JS and Tofilon PJ (2002) Radiation-induced activation of nuclear factor-kappaB involves selective degradation of plasma membrane-associated I(kappa-)B(alpha). *Mol Biol Cell* **13:**3431–3440.

Shojaei F, Gallacher L, and Bhatia M (2004) Differential gene expression of human stem progenitor cells derived from early stages of in utero human hematopoiesis. *Blood* **103:**2530–2540.

Singh VK, Shafran RL, Inal CE, Jackson WE 3rd, and Whitnall MH (2005) Effects of whole-body gamma irradiation and 5-androstenediol administration on serum G-CSF. *Immunopharmacol Immunotoxicol* **27:**521–534.

Stickney DR, Dowding C, Authier S, Garsd A, Onizuka-Handa N, Reading C, and Frincke JM (2007) 5-androstenediol improves survival in clinically unsupported rhesus monkeys with radiation-induced myelosuppression. *Int Immunopharmacol* **7:**500–505.

Stickney DR, Dowding C, Garsd A, Ahlem C, Whitnall M, McKeon M, Reading C, and Frincke J (2006) 5-androstenediol stimulates multilineage hematopoiesis in rhesus monkeys with radiation-induced myelosuppression. *Int Immunopharmacol* **6:**1706–1713.

Szalay L, Shimizu T, Suzuki T, Hsieh YC, Choudhry MA, Schwacha MG, Bland KI, and Chaudry IH (2006) Androstenediol administration after trauma-hemorrhage attenuates inflammatory response, reduces organ damage, and improves survival following sepsis. *Am J Physiol Gastrointest Liver Physiol* **291:**G260–G266.

Thompson JE, Phillips RJ, Erdjument-Bromage H, Tempst P, and Ghosh S (1995) I kappa B-beta regulates the persistent response in a biphasic activation of NF-kappa B. *Cell* **80:**573–582.

Vanden Berghe W, Vermeulen L, De Wilde G, De Bosscher K, Boone E, and Haegeman G (2000) Signal transduction by tumor necrosis factor and gene regulation of the inflammatory cytokine interleukin-6. *Biochem Pharmacol* **60:**1185–1195.

Whitnall MH, Elliott TB, Harding RA, Inal CE, Landauer MR, Wilhelmsen CL, McKinney L, Miner VL, Jackson WE, Loria RM, et al. (2000) Androstenediol stimulates myelopoiesis and enhances resistance to infection in gamma-irradiated mice. *Int J Immunopharmacol* **22:**1–14.

Whitnall MH, Villa V, Seed TM, Benjack J, Miner V, Lewbart ML, Dowding CA, and Jackson WE, 3rd (2005) Molecular specificity of 5-androstenediol as a systemic radioprotectant in mice. *Immunopharmacol Immunotoxicol* **27:**15–32.

Xiao M, Oppenlander BK, and Dooley DC (2001) Transforming growth factor-beta$_1$ induces apoptosis in CD34$^+$CD38$^{-/low}$ cells that express Bcl-2 at a low level. *Exp Hematol* **29:**1098–1108.

Zhou D, Yu T, Chen G, Brown SA, Yu Z, Mattson MP, and Thompson JS (2001) Effects of NF-kappaB1 (p50) targeted gene disruption on ionizing radiation-induced NF-kappaB activation and TNFalpha, IL-1alpha, IL-1beta and IL-6 mRNA expression in vivo. *Int J Radiat Biol* **77:**763–772.

Address correspondence to: Dr. Mang Xiao, Armed Forces Radiobiology Research Institute, 8901 Wisconsin Ave., Bethesda, MD 20889-5603. E-mail: xiao@afrri.usuhs.mil